

# Kinetic Analysis of Electron Transfer across Single Water-Microdroplet/Oil and Oil-Microdroplet/Water Interfaces

Kiyoharu NAKATANI,<sup>\*†</sup> Mitsuharu UCHINO,<sup>\*</sup> Shingo SUZUKI,<sup>\*</sup> Takayuki NEGISHI,<sup>\*</sup> and Toshiyuki OSAKAI<sup>\*\*</sup>

<sup>\*</sup>Department of Chemistry, Graduate School of Pure and Applied Sciences, University of Tsukuba, Tsukuba, Ibaraki 305-8571, Japan

<sup>\*\*</sup>Department of Chemistry, Graduate School of Science, Kobe University, Kobe, Hyogo 657-8501, Japan

Using techniques comprising laser trapping, microcapillary injection/manipulation, fluorescence microspectroscopy and electrochemistry of single microdroplets, we kinetically investigated the electron transfer (ET) reaction between decamethylferrocene in tributyl phosphate and hexacyanoferrate(III) in water. In the oil-microdroplet/water system, the overall ET reaction rate significantly depended on the droplet radius ( $r_d$ ,  $0.5 \mu\text{m} < r_d < 10 \mu\text{m}$ ) and on the potential-determining ion concentration in the oil phase. The interfacial ET reaction rate constant determined in the water-microdroplet ( $r_d = 21 \mu\text{m}$ )/oil system agreed very well with that in the oil-microdroplet ( $r_d > 2 \mu\text{m}$ )/water system. The rate constant values were extremely small in the Gibbs free energy ( $\Delta G$ ) range of  $-10$  to  $-25 \text{ kJ mol}^{-1}$ , with  $\Delta G$  consisting of the Galvani potential difference between the water and oil phases and the redox potential difference of the solutes. The characteristic ET reaction was discussed in terms of the ion transfer and the ET across the interfacial mixed layer with nanometer-sized thickness.

(Received August 27, 2008; Accepted October 6, 2008; Published February 10, 2009)

## Introduction

Electron transfer (ET) and ion transfer across an oil/water interface are important fundamental processes for understanding the chemical and physical processes in oil-in-water or water-in-oil emulsions and the like. ET reactions across liquid/liquid interfaces have been electrochemically and spectroscopically studied using polarized or non-polarized liquid/liquid interface systems.<sup>1-12</sup> We have reported an ET reaction between a ferrocene derivative such as decamethylferrocene (dcmFc) in tributyl phosphate (TBP) microdroplets and  $\text{Fe}(\text{CN})_6^{3-}$  in water by using a technique comprising laser trapping, electrochemistry and microspectroscopy.<sup>13,14</sup> The overall ET reaction rate constant (per unit interfacial area) between dcmFc and  $\text{Fe}(\text{CN})_6^{3-}$  was independent of the droplet radius ( $r_d$ ) greater than  $5 \mu\text{m}$ , while it decreased with decreasing  $r_d$  in the range smaller than  $5 \mu\text{m}$ .<sup>14</sup> In the oil-microdroplet/water system, however, the volume of the oil phase was much smaller than that of the water phase, so that the decamethylferrocenium cation ( $\text{dcmFc}^+$ ) generated in the oil microdroplet would exit into the water phase.<sup>15,16</sup> In that report, therefore, the peculiar droplet size dependence of the ET reaction could not be explained in detail.

Recently, we have developed an electrochemical method combined with a microcapillary injection/manipulation technique and then analyzed the ET reaction between  $\text{Fe}(\text{CN})_6^{3-}$  in a single water microdroplet and dcmFc in 2-nitrophenyl octyl ether (NPOE).<sup>17</sup> In the single water-microdroplet/oil system,  $\text{dcmFc}^+$  would not distribute into the water phase due to the

large volume ratio of the oil to the water phase. The overall ET rate could be successfully discussed on the basis of the dependence on the Gibbs free energy ( $\Delta G$ ). In the present article, we examine the ET reaction between dcmFc in TBP and  $\text{Fe}(\text{CN})_6^{3-}$  in water based on the characteristics of the ion transfer in the single water-microdroplet and oil-microdroplet systems and we discuss the ET and the ion transfer across the water/TBP interface in detail.

## Experimental

### Materials

Potassium hexacyanoferrate(II) (Wako Pure Chemical Industries, 99.5%), dcmFc (Aldrich, 99+%), tetraalkylammonium chloride (TAACl; tetrapropylammonium ( $\text{TPrA}^+$ , Aldrich, 98%), tetrabutylammonium ( $\text{TBA}^+$ , Tokyo Kasei Kogyo, GR grade)), and potassium chloride (Kishida Reagent Chemicals, >99.5%) were purified by recrystallizations from water, methanol, acetone-diethyl ether, and water, respectively. Perylene (Pe, Janssen Chimica, 99+%) was used without further purification. Tetraalkylammonium tetraphenylborate (TAATPB) was prepared from TAACl and sodium tetraphenylborate (Aldrich, Inc., 99.5+%), and then purified by recrystallizations from acetone. Water was used after deionization and distillation (Yamato Scientific, Autostill WG221). Tributyl phosphate (TBP) (Tokyo Kasei Kogyo, >99.0%) was purified by washing with water.

### Single microdroplet measurements

Single water microdroplet measurements were performed by a microcapillary manipulation-electrochemistry technique (Fig. 1).<sup>17</sup> A TBP-saturated aqueous solution ( $20 \text{ cm}^3$ ) of TAACl (10 mM)

<sup>†</sup> To whom correspondence should be addressed.  
E-mail: nakatani@chem.tsukuba.ac.jp

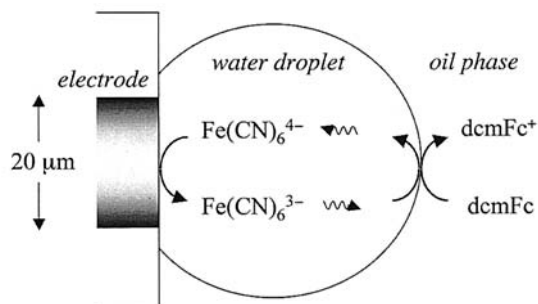


Fig. 1 Schematic illustration of a single water-microdroplet/TBP system.

and KCl (90 mM) was poured into a glass dish. A glass plate (10 × 10 × 1 mm) treated with dichlorodimethylsilane was placed on the bottom of the glass dish. A water-saturated TPB solution (0.2 cm<sup>3</sup>) of dcmFc (0 or 5 mM) and TAATPB (10 or 30 mM) was injected onto the glass plate. A Pt micro-disk-electrode of 20 μm diameter fabricated in a glass microcapillary (tip diameter of ~50 μm) was used as the working electrode. The working electrode was inserted into the TBP phase and a TBP-saturated single water microdroplet ( $r_d = 21 \pm 1 \mu\text{m}$ ) containing K<sub>4</sub>Fe(CN)<sub>6</sub> (1 mM), TAACl (10 mM) and KCl (80 mM) was contacted with the microelectrode using a microcapillary manipulation and injection system (Narishige, MN-151/IM-16) under an optical microscope (Nikon, SMZ-U). The single water microdroplet completely covered the microelectrode surface. Reference (Ag/AgCl) and counter (Pt wire) electrodes were positioned in the outer water phase. Electrochemical measurements of the single water droplets were performed at 294 K using an electrochemical analyzer (BAS, BAS100B/W) and a temperature controller (Tokai Kit, MATS-555NSL).

Single oil microdroplet measurements were performed by a laser trapping-spectroscopy-electrochemistry technique (Fig. 2).<sup>13,14</sup> Water-saturated TBP containing dcmFc (20 mM), Pe (0.5 mM), and TAATPB (10 or 30 mM) was vigorously mixed in TBP-saturated water of TAACl (1 – 90 mM), KCl, and K<sub>4</sub>Fe(CN)<sub>6</sub> (0.2 mM) with a 1/500 (oil/water) weight ratio. The ionic strength of the water phase was adjusted to 90 mM with KCl. The sample emulsion was placed between an SnO<sub>2</sub> working electrode and a cover glass with a Teflon film (50 μm thickness) on the stage of an optical microscope (Olympus, BX-60). Pt and Ag/AgCl electrodes were used as the counter and reference electrodes, respectively. A 1064-nm beam from a CW Nd<sup>3+</sup>:YVO<sub>4</sub> laser (Spectra-Physics, Millennia IR) was introduced into the optical microscope and focused onto a single microdroplet (0.5 μm <  $r_d$  < 10 μm) for laser trapping. Bulk electrolysis was performed by the electrochemical analyzer. A 406-nm beam from a diode laser (Neoark, TC20-40305-2F4.5) was irradiated on the laser-trapped droplet and the fluorescence from the droplet was analyzed by a multichannel photodetector (Andor Technology, DV401-BV). All measurements were performed at 294 K.

## Results

### Single water microdroplet measurements

As shown in Fig. 1, Fe(CN)<sub>6</sub><sup>4-</sup> was oxidized to Fe(CN)<sub>6</sub><sup>3-</sup> at the working electrode/water-microdroplet interface and the generated Fe(CN)<sub>6</sub><sup>3-</sup> was reduced to Fe(CN)<sub>6</sub><sup>4-</sup> by dcmFc at the water-microdroplet/oil interface. The diffusion time of

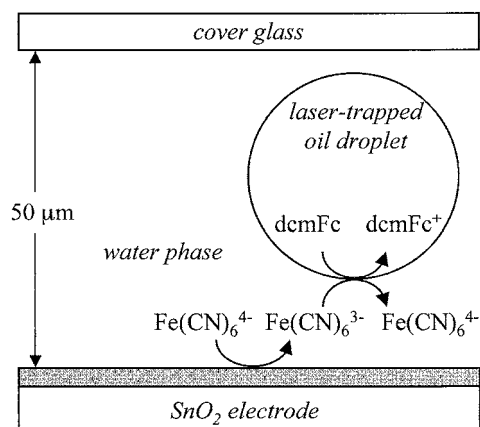


Fig. 2 Schematic illustration of a single TBP-microdroplet/water system.

Fe(CN)<sub>6</sub><sup>4-</sup>/Fe(CN)<sub>6</sub><sup>3-</sup> between the electrode interface and the microdroplet/oil interface is short because of the micrometer-sized droplet. A current flowing through the working electrode should increase with the ET rate at the water-microdroplet/oil interface, which is affected by the  $\Delta G$  of the ET reaction. The  $\Delta G$  is dependent on the Galvani potential difference between the water and TBP phases ( $\Delta\phi$ ); however, in the present water/TBP system, the absolute values of  $\Delta\phi$  cannot be estimated, because no literature values are available for the standard ion transfer potentials of the potential-determining ions (probably TAA<sup>+</sup>). Nonetheless, the  $\Delta G$  of ET between Fe(CN)<sub>6</sub><sup>3-</sup> and dcmFc can be obtained using the relation:  $-\Delta G = F(E_{\text{Fe(CN)}_6^{3-}/\text{Fe(CN)}_6^{4,w}} - E_{\text{dcmFc}^+/\text{dcmFc}}^{0,o} + \Delta\phi)$ , where  $E_{\text{Fe(CN)}_6^{3-}/\text{Fe(CN)}_6^{4,w}}$  and  $E_{\text{dcmFc}^+/\text{dcmFc}}^{0,o}$  are the formal potentials of Fe(CN)<sub>6</sub><sup>3-</sup>/Fe(CN)<sub>6</sub><sup>4-</sup> in water and dcmFc<sup>+</sup>/dcmFc in TBP, respectively.<sup>17</sup>  $F$  is the Faraday constant. The formal redox potential of dcmFc<sup>+</sup>/dcmFc in TBP versus the reference electrode in water ( $E_{\text{dcmFc}^+/\text{dcmFc}}^{0,w}$ ) is given by  $E_{\text{dcmFc}^+/\text{dcmFc}}^{0,o} - \Delta\phi$ . Since the  $\Delta\phi$  between the water droplet and TBP is the same as that between the outer water and the TBP under the present experimental conditions,  $E_{\text{dcmFc}^+/\text{dcmFc}}^{0,w}$  can be evaluated from a cyclic voltammogram (CV) of dcmFc without a water microdroplet. Thus,  $\Delta G$  was experimentally estimated from  $-\Delta G = F(E_{\text{Fe(CN)}_6^{3-}/\text{Fe(CN)}_6^{4,w}} - E_{\text{dcmFc}^+/\text{dcmFc}}^{0,w})$ .

Figure 3 shows the CVs of Fe(CN)<sub>6</sub><sup>4-</sup> in single water microdroplets in the absence and presence of dcmFc in the TBP phase. In the absence of dcmFc, the CV was a symmetrical peaked curve, since Fe(CN)<sub>6</sub><sup>4-</sup> and the generated Fe(CN)<sub>6</sub><sup>3-</sup> were completely electrolyzed during the potential sweep. In the presence of dcmFc, on the other hand, the CV was a sigmoidal curve and the limiting current ( $i_{\text{lim}}$ ) increased with the increasing  $\Delta G$ . Using the diffusion coefficient ( $D$ ) of dcmFc in TBP ( $1.6 \times 10^{-6} \text{ cm}^2 \text{ s}^{-1}$ ), we estimated a diffusion-limited steady-state current ( $i_{\text{ss}}$ ) without the water microdroplet to be 3 nA by the equation:  $i_{\text{ss}} = 4FDC_0r_e$ ,<sup>18</sup> where  $C_0$  and  $r_e$  are the dcmFc concentration in TBP (5 mM) and the radius of the micro-disk-electrode (10 μm), respectively. The  $i_{\text{lim}}$  value was much smaller than the  $i_{\text{ss}}$  value. Therefore, the ET at the water-microdroplet/oil interface is suggested to be slow compared with the diffusion of dcmFc.

As reported previously, the CV was analyzed on the basis of digital simulations using a cylindrical diffusion equation of radially- ( $r$ ) and perpendicularly-directed ( $z$ ) coordinates.<sup>17</sup> A water droplet shape was approximated as a cylinder ( $r_c$ , radius;  $z_c$ , length). The  $r_c$  and  $z_c$  values were determined as the volume of the droplet with  $z_d$  (observed distance between the electrode

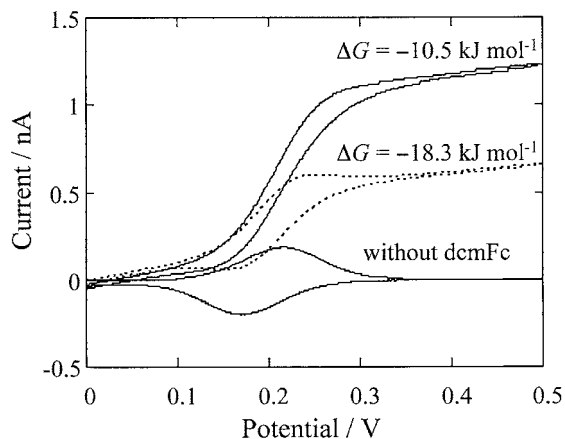


Fig. 3 Cyclic voltammograms ( $5 \text{ mV s}^{-1}$ ) of  $\text{Fe}(\text{CN})_6^{4-}$  in single water microdroplets of  $r_d = 21 \pm 1 \mu\text{m}$  at  $[\text{TBA}^+]_o = [\text{TBA}^+]_w = 10 \text{ mM}$  ( $\Delta G = -10.5 \text{ kJ mol}^{-1}$ ),  $[\text{TPrA}^+]_o = [\text{TPrA}^+]_w = 10 \text{ mM}$  ( $\Delta G = -18.3 \text{ kJ mol}^{-1}$ ), and  $[\text{TBA}^+]_o = [\text{TBA}^+]_w = 10 \text{ mM}$  in the absence of dcmFc.

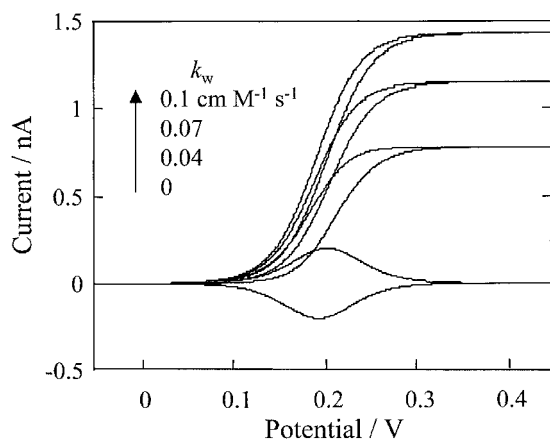


Fig. 4 Cyclic voltammograms of  $\text{Fe}(\text{CN})_6^{4-}$  in a single water microdroplet at  $5 \text{ mV s}^{-1}$  simulated for various  $k_w$  values.

and the water droplet/TBP interface normal to the electrode surface) was equal to that of the cylinder under the condition of  $r_d/z_c = r_d/z_d$ . In the simulations,  $7.0 \times 10^{-6}$  and  $1.6 \times 10^{-6} \text{ cm}^2 \text{ s}^{-1}$  were used as the  $D$  values for  $\text{Fe}(\text{CN})_6^{4-}/\text{Fe}(\text{CN})_6^{3-}$  in water and dcmFc/dcmFc<sup>+</sup> in TBP, respectively. We assumed that the electrode reaction is reversible and we excluded mass transfer of the redox species between the water and TBP phases. The cyclic voltammograms were then simulated by an explicit finite differential method under the conditions of  $\Delta r = \Delta z = 0.5 \mu\text{m}$  and  $D\Delta t/\Delta r^2 < 0.23$  for various values of the interfacial rate constant ( $k_w$ ) at the water/TBP interface (Fig. 4). In the absence of dcmFc, the peak current of the simulated CV agreed very well with that of the observed one, although the observed CV was slightly irreversible. In the presence of dcmFc, the simulated  $i_{\text{lim}}$  value increased with the increasing  $k_w$ . From the comparison between the simulated and observed values of  $i_{\text{lim}}$ , the  $k_w$  value for the observed CV was determined to be  $10^{-2}$ – $10^{-1} \text{ cm M}^{-1} \text{ s}^{-1}$  at  $\Delta G = -10$  to  $-20 \text{ kJ mol}^{-1}$ .

#### Single oil microdroplet measurements

A single TBP microdroplet was laser-trapped in the thin-layer electrolytic cell without direct contact with the electrode or the

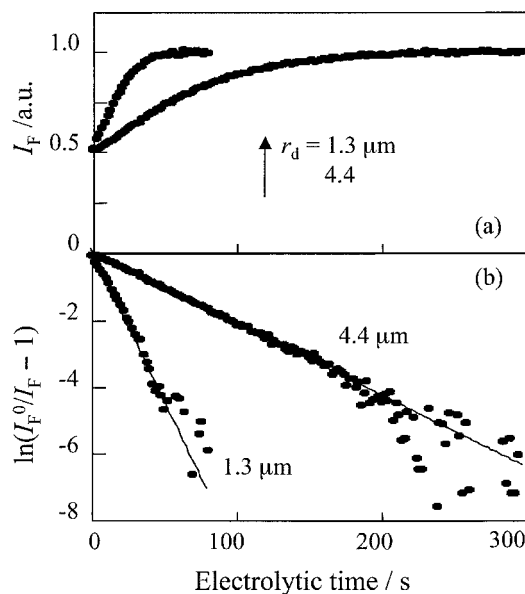


Fig. 5 Electrolytic time dependencies of (a)  $I_F$  and (b)  $\ln(I_F^0/I_F - 1)$  in single TBP microdroplets with  $r_d = 1.3$  and  $4.4 \mu\text{m}$  for  $30 \text{ mM}$  TPrATPB and  $1 \text{ mM}$  TPrACl ( $\Delta G = -23.3 \text{ kJ mol}^{-1}$ ).

cover glass.  $\text{Fe}(\text{CN})_6^{4-}$  in the water phase was oxidized by potential-controlled bulk electrolysis at  $0.8 \text{ V}$  (vs.  $\text{Ag}/\text{AgCl}$ ). As one characteristic of bulk electrolysis in the thin-layer cell with a gap of  $50 \mu\text{m}$ ,  $\text{Fe}(\text{CN})_6^{4-}$  is completely electrolyzed to  $\text{Fe}(\text{CN})_6^{3-}$  within  $\sim 10 \text{ s}$  by the bulk electrolysis. Therefore, the  $\text{Fe}(\text{CN})_6^{3-}$  concentration in water ( $[\text{Fe}(\text{CN})_6^{3-}]_w$ ) is assumed to be  $0.2 \text{ mM}$  at the electrolytic time ( $t$ ) greater than  $\sim 10 \text{ s}$ .<sup>18</sup> Then, the ET between dcmFc in the droplet and  $\text{Fe}(\text{CN})_6^{3-}$  in the water phase was induced (Fig. 2). Fluorescence of Pe in the droplet is quenched by dcmFc, so that the dcmFc concentration in the droplet ( $[\text{dcmFc}]_o$ ) can be determined from the fluorescence intensity ( $I_F$ ) based on the Stern-Volmer relation:  $I_F^0/I_F = 1 + k_q \tau_0 [\text{dcmFc}]_o$ , where  $I_F^0$ ,  $k_q$  and  $\tau_0$  are, respectively, the  $I_F$  at  $[\text{dcmFc}]_o = 0$ , the fluorescence quenching rate constant of Pe by dcmFc ( $7.3 \times 10^9 \text{ M}^{-1} \text{ s}^{-1}$ ) and the fluorescence lifetime of Pe without dcmFc ( $4.7 \text{ ns}$ ).<sup>14</sup>

Figure 5a shows the time dependence of  $I_F$  of the single droplets. The diffusion time of dcmFc between the microdroplet interior and the droplet surface is very short, and the mass transfer between the microdroplet surface and the bulk water phase is fast due to the steady-state spherical diffusion. Therefore, when the interfacial process at the oil microdroplet/water boundary is the rate-determining step of the overall ET reaction, the reaction rate at  $t > 10 \text{ s}$  can be analyzed on the basis of a pseudo-first-order kinetic equation ( $[\text{Fe}(\text{CN})_6^{3-}]_w = 0.2 \text{ mM}$ ):  $\ln[\text{dcmFc}]_o/[\text{dcmFc}]_{o,0} = -k[\text{Fe}(\text{CN})_6^{3-}]_w t$ , where  $[\text{dcmFc}]_{o,0}$  and  $k$  are, respectively, the  $[\text{dcmFc}]_o$  at  $t = 0$  and the observed rate constant. Combining this equation with the Stern-Volmer equation, we obtain the kinetic equation:  $\ln(I_F^0/I_F - 1) = -k[\text{Fe}(\text{CN})_6^{3-}]_w t + \ln(k_q \tau_0 [\text{dcmFc}]_{o,0})$ .<sup>13</sup> As shown in Fig. 5b, the  $\ln(I_F^0/I_F - 1)$  value was proportional to  $t$ , indicating that the reaction rate is governed by the interfacial process. The  $k$  value was calculated from the slope of the plot. The error in determining  $k$  was estimated to be  $\pm 10\%$ .

The interfacial reaction rate constant ( $k_o$ ) is dependent on the interfacial area ( $4\pi r_d^2$ )/volume ( $(4/3)\pi r_d^3$ ) ratio of the microdroplet and is given by  $k = \{4\pi r_d^2/(4/3)\pi r_d^3\} k_o = (3/r_d) k_o$ .<sup>13</sup> Indeed,  $k$  increased with decreasing  $r_d$  (Fig. 5). Figure 6 shows the  $r_d$  dependence of  $k$  for  $[\text{TPrA}^+]_o/[\text{TPrA}^+]_w = 1/3$  ( $[\text{TAA}^+]_o$ ,

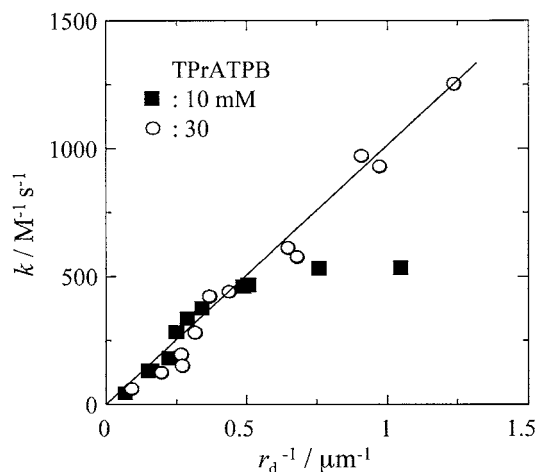


Fig. 6  $k$  for various  $r_d$  values at TPrATPB of 10 and 30 mM ( $[\text{TPrA}^+]_o/[\text{TPrA}^+]_w = 1/3$ ,  $\Delta G = -8.2 \text{ kJ mol}^{-1}$ ).

TAA<sup>+</sup> concentration in TBP;  $[\text{TAA}^+]_w$ , TAA<sup>+</sup> concentration in water). Provided that the potential-determining ion is TPrA<sup>+</sup> in this system, the  $\Delta\phi$  for  $[\text{TPrA}^+]_o/[\text{TPrA}^+]_w = 30 \text{ mM}/90 \text{ mM}$  should coincide with that for  $[\text{TPrA}^+]_o/[\text{TPrA}^+]_w = 10 \text{ mM}/30 \text{ mM}$  according to the Nernst equation.  $k$  was directly proportional to  $r_d^{-1}$  for 30 mM TPrATPB. The  $k$  for 10 mM TPrATPB agreed very well with that for 30 mM TPrATPB at  $r_d > 2 \mu\text{m}$ , while the linear relationship for 10 mM TPrATPB deviated at  $r_d < 2 \mu\text{m}$ . A deviation from the linear relationship was observed at  $[\text{TAA}^+]_o = 10 \text{ mM}$  for various  $[\text{TAA}^+]_w$  values. In the  $\Delta G$  range of  $-10$  –  $-25 \text{ kJ mol}^{-1}$ , the  $k_o$  values were determined to be  $10^{-2}$  –  $10^{-1} \text{ cm M}^{-1} \text{ s}^{-1}$  at  $r_d > 2 \mu\text{m}$ .

## Discussion

### Dependence of $k$ on $r_d$ in the oil microdroplet system

Previously, we have reported that  $k$  is directly proportional to  $r_d^{-1}$  at  $r_d > 5 \mu\text{m}$  but saturated at  $r_d < 5 \mu\text{m}$  when using TBA<sup>+</sup> as a potential-determining ion between the TBP and water phases.<sup>14</sup> The overall ET rate was only analyzed for 10 mM TBATPB, since TBATPB does not dissolve greater than 10 mM in TBP. In that report, we speculated that the  $r_d$  dependence of  $k$  originated from the ET reaction in a thick interfacial layer. As characteristics of chemical and physical processes in microdroplet/solution systems, when a rate constant is proportional to  $r_d^{-1}$  or  $r_d^{-2}$ , the rate-determining step is the process at the microdroplet/solution interface or the diffusion between the microdroplet/solution interface and the bulk solution phase, respectively.<sup>19</sup> If the rate constant is independent of  $r_d$ , the rate-determining step is the process in the bulk solution phase. According to this  $r_d$  dependence, the thickness of the TBP/water interface may be  $\sim 2 \mu\text{m}$  at 10 mM TPrATPB (or TBATPB) and smaller than  $\sim 0.5 \mu\text{m}$  at 30 mM TPrATPB (Fig. 6). In this case, the overall ET rate constant should depend on the thickness of the interfacial layer. However,  $k_o$  ( $0.03 \text{ cm M}^{-1} \text{ s}^{-1}$ ) determined from the  $k$  values at  $r_d > 2 \mu\text{m}$  for 10 mM TPrATPB agreed very well with that for 30 mM TPrATPB. In the water-microdroplet/oil system, furthermore,  $k_w$  ( $0.02$  –  $0.03 \text{ cm M}^{-1} \text{ s}^{-1}$ ) was independent of the TPrATPB concentration. Therefore, these results cannot be explained by the assumption of the interfacial layer with micrometer-sized thickness. For 10 mM TAA<sup>+</sup> in the TBP droplet ( $[\text{dcmFc}]_o = 20 \text{ mM}$ ), since  $k$  is smaller for larger droplets, the amount of dcmFc<sup>+</sup> produced at

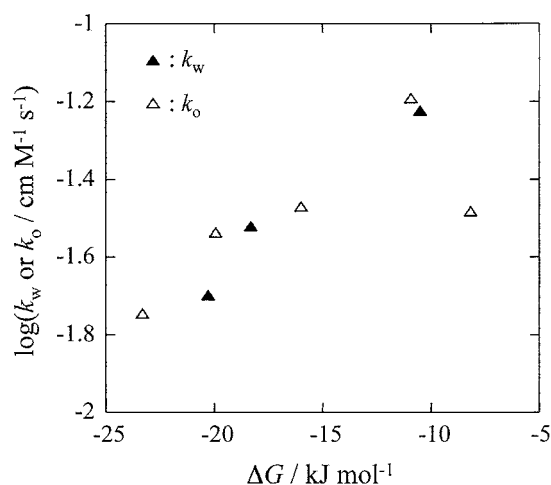


Fig. 7  $\Delta G$  dependencies of  $k_w$  and  $k_o$ .

the droplet/water interface per unit time is less than that of TAA<sup>+</sup> in the diffusion layer from the interface to the droplet interior. Thus, the interfacial ET and ion transfer proceed at the  $\Delta\phi$  value determined primarily by the TAA<sup>+</sup> concentrations in the two phases during the sample preparation. For smaller droplets, on the other hand, the amount of dcmFc<sup>+</sup> produced at the droplet/water interface per unit time is greater than that of TAA<sup>+</sup> in the diffusion layer.  $k$  deviated from the linear relationship, probably because the  $\Delta\phi$  value would change during the interfacial ET reaction.

### Slow ET reaction across water/TBP interface

Figure 7 shows the  $\Delta G$  dependence of  $k_w$  and  $k_o$ . Using the single water microdroplet technique,  $k_w$  has been reported to be  $\sim 10 \text{ cm M}^{-1} \text{ s}^{-1}$  at  $\Delta G \sim -15 \text{ kJ mol}^{-1}$  in a water/NPOE system.<sup>17</sup> The  $k_w$  values in the water/TBP system are much smaller than those in the water/NPOE system. The ET rate constants between dcmFc and  $\text{Fe}(\text{CN})_6^{3-}$  across liquid/liquid interfaces have been reported to be greater than  $10^{-1} \text{ cm M}^{-1} \text{ s}^{-1}$  ( $\Delta G < 0$ ) by other techniques.<sup>4,5,8</sup> Furthermore, if the overall ET reaction is governed by the interfacial ET process, the ET rate constant should increase with decreasing  $\Delta G$ . However,  $k_w$  and  $k_o$  slightly decreased with the decreasing  $\Delta G$ . These results indicate that the ET between dcmFc and  $\text{Fe}(\text{CN})_6^{3-}$  in the water/TBP system is different from that in the liquid/liquid system such as the water/NPOE system.

Ion transfer across the water/TBP interface is coupled with the ET between dcmFc and  $\text{Fe}(\text{CN})_6^{3-}$ , being dependent on  $\Delta\phi$ .  $\text{Fe}(\text{CN})_6^{4-}$  and  $\text{Fe}(\text{CN})_6^{3-}$  in water will not distribute into TBP. It has been reported that dcmFc in TBP does not distribute into water while dcmFc<sup>+</sup> distributes from TBP into water at analogous  $\Delta\phi$  values.<sup>15,16</sup> In the TBP-microdroplet/water system, the dcmFc<sup>+</sup> molecules easily distribute from the oil microdroplet into water under the present experimental conditions, because of the small volume ratio of the oil to the water. The dcmFc<sup>+</sup> distributed in the water phase will react with  $\text{Fe}(\text{CN})_6^{4-}$ . In the water-microdroplet/oil system, on the other hand, the volume ratio of the water microdroplet to the oil was extremely small, so that few dcmFc<sup>+</sup> molecules distribute into the water phase. Nonetheless,  $k_w$  was in good agreement with  $k_o$  for analogous  $\Delta G$  and thus  $\Delta\phi$ . We conclude that the rate-determining step of the overall ET reaction is not limited by the ion transfer between the two bulk phases.

*ET in interfacial mixed layer with nanometer-sized thickness*

The thickness of a water/nitrobenzene or water/1,2-dichloroethane interface has been reported to be ~1 nm.<sup>20-22</sup> Although the water/nitrobenzene or water/1,2-dichloroethane interface can be easily polarized, the water/TBP interface was not well polarized using a four-electrode electrochemical technique. Furthermore, the solubility of water in TBP (4.67 wt%) is much larger than that in nitrobenzene (0.24 wt%) or 1,2-dichloroethane (0.15 wt%).<sup>23</sup> Therefore, we consider that an interfacial mixed layer with thickness greater than ~1 nm (though smaller than ~0.5  $\mu\text{m}$ ) exists in the water/TBP system, so that the overall ET rate may be extremely slow. In the interfacial mixed layer, the “effective” potential difference responsible for the ET reaction seems to be rather small. Therefore, the contribution of  $\Delta\% \phi$  to  $\Delta G$  will be small. Since the ET reaction proceeded in the absence of TAATPB in the TBP droplet,<sup>14</sup> it can be speculated that both dcmFc and  $\text{Fe}(\text{CN})_6^{3-}$  distribute in the interfacial layer. A previous study<sup>24</sup> showed that the  $k_0$  for dcmFc/ $\text{Fe}(\text{CN})_6^{3-}$  in the TBP-microdroplet/water system was close to that for ferrocene/ $\text{Fe}(\text{CN})_6^{3-}$  ( $10^{-2} \text{ cm M}^{-1} \text{ s}^{-1}$ ) at analogous  $\Delta\% \phi$  values. The redox potential of dcmFc<sup>+</sup>/dcmFc (0.11 V vs. Ag in TBP) is much smaller than that of ferrocenium/ferrocene (0.51 V vs. Ag in TBP).<sup>14</sup> Furthermore, dcmFc<sup>+</sup>/dcmFc is highly hydrophobic compared with ferrocenium/ferrocene. Therefore, the overall ET rate will not be governed by the ET between dcmFc and  $\text{Fe}(\text{CN})_6^{3-}$  in the interfacial layer and the mass transfer rate of dcmFc<sup>+</sup>/dcmFc between the interfacial layer and the TBP phase. We consider that the rate-determining step of the overall ET reaction is the mass transfer of  $\text{Fe}(\text{CN})_6^{3-}$  between the interfacial mixed layer and the water phase.

**Conclusions**

The ET reaction between dcmFc in TBP and  $\text{Fe}(\text{CN})_6^{3-}$  in water was analyzed by measurements in the single water-microdroplet/oil and oil-microdroplet/water systems. In the oil-microdroplet/water system, the concentration of dcmFc<sup>+</sup> was comparable with that of TAA<sup>+</sup> in the microdroplet. The ET reaction was thus coupled with the transfer of dcmFc<sup>+</sup> and TAA<sup>+</sup> between the TBP and water phases, so that a peculiar  $r_d$  dependence of  $k$  was observed at  $r_d < 2 \mu\text{m}$ . The overall ET reaction rate was extremely slow in the water-microdroplet/oil and oil-microdroplet/water ( $r_d > 2 \mu\text{m}$ ) systems and the rate-determining step was not the ET at the water/TBP interface and the ion transfer between the bulk two phases. These results suggested a possible rate-determining ET reaction in the interfacial mixed layer with nanometer-sized thickness.

**Acknowledgements**

K. N. is grateful for a Grant-in-Aid for Scientific Research of Priority Areas (No. 13129202) from the Ministry of Education,

Culture, Sports, Science and Technology for partial support of this study.

**References**

1. Z. Samec, V. Marecek, and J. Weber, *J. Electroanal. Chem.*, **1979**, *96*, 245.
2. G. Geblewicz and D. J. Schiffrin, *J. Electroanal. Chem.*, **1988**, *244*, 27.
3. B. Liu and M. V. Mirkin, *J. Am. Chem. Soc.*, **1999**, *121*, 8352.
4. C. Shi and F. C. Anson, *J. Phys. Chem. B*, **1998**, *102*, 9850.
5. C. Shi and F. C. Anson, *J. Phys. Chem. B*, **2001**, *105*, 8963.
6. A. L. Barker, P. R. Unwin, S. Amemiya, J. Zhou, and A. J. Bard, *J. Phys. Chem. B*, **1999**, *103*, 7260.
7. J. Zhang and P. R. Unwin, *J. Phys. Chem. B*, **2000**, *104*, 2341.
8. J. Zhang, A. L. Barker, and P. R. Unwin, *J. Electroanal. Chem.*, **2000**, *483*, 95.
9. Z. Zhang, Y. Yuan, P. Sun, B. Su, J. Guo, Y. Shao, and H. H. Girault, *J. Phys. Chem. B*, **2002**, *106*, 6713.
10. M. Suzuki, S. Umetani, M. Matsui, and S. Kihara, *J. Electroanal. Chem.*, **1997**, *420*, 119.
11. H. Hotta, S. Ichikawa, T. Sugihara, and T. Osakai, *J. Phys. Chem. B*, **2003**, *107*, 9717.
12. T. Osakai, S. Ichikawa, H. Hotta, and H. Nagatani, *Anal. Sci.*, **2004**, *20*, 1567.
13. K. Nakatani, K. Chikama, H.-B. Kim, and N. Kitamura, *Chem. Phys. Lett.*, **1995**, *237*, 133.
14. K. Chikama, K. Nakatani, and N. Kitamura, *Bull. Chem. Soc. Jpn.*, **1998**, *71*, 1065.
15. K. Nakatani and T. Negishi, *Rev. Polarogr.*, **2001**, *47*, 88.
16. K. Nakatani, T. Sekine, and T. Negishi, “*Encyclopedia of Surface and Colloid Science*”, ed. A. Hubbard, **2002**, Vol. 3, Marcel Dekker, New York, 3391.
17. K. Nakatani, J. Yamashita, T. Negishi, and T. Osakai, *J. Electroanal. Chem.*, **2005**, *575*, 27.
18. A. J. Bard and L. R. Faulkner, “*Electrochemical Methods: Fundamentals and Applications*”, **2001**, John Wiley and Sons, New York, Chichester, Weinheim, Brisbane, Singapore, Toronto.
19. T. H. James, “*The Theory of the Photographic Process*”, **1977**, Macmillan, New York.
20. I. Benjamin, *Chem. Rev.*, **1996**, *96*, 1449.
21. Y. Cheng and D. J. Schiffrin, *J. Chem. Soc. Faraday Trans.*, **1993**, *89*, 199.
22. H. H. Girault and D. J. Schiffrin, *J. Electroanal. Chem.*, **1983**, *150*, 43.
23. J. A. Riddick and W. B. Bunger, “*Techniques of Chemistry: Organic Solvent*”, **1970**, Vol. 2, Wiley-Interscience, New York.
24. K. Chikama, K. Nakatani, and N. Kitamura, *Chem. Lett.*, **1996**, 665.